Human Molecular Genetics, 2013, Vol. 22, No. 3 ***519–530***
doi:10.1093/hmg/dds450
Advance Access published on October 25, 2012

ORMDL3 modulates store-operated calcium entry and lymphocyte activation

Amado Carreras-Sureda[1,†], Gerard Cantero-Recasens[1,†], Fanny Rubio-Moscardo[1], Kerstin Kiefer[1], Christine Peinelt[2], Barbara A. Niemeyer[2], Miguel A. Valverde[1] and Rubén Vicente[1,*]

[1]Laboratory of Molecular Physiology and Channelopathies, Department of Experimental and Health Sciences, Universitat Pompeu Fabra, Barcelona 08003, Spain and [2]Department of Biophysics, University of Saarland, Homburg 66421, Germany

Received September 21, 2012; Revised and Accepted October 18, 2012

T lymphocytes rely on a Ca^{2+} signal known as store-operated calcium entry (SOCE) for their activation. This Ca^{2+} signal is generated by activation of a T-cell receptor, depletion of endoplasmic reticulum (ER) Ca^{2+} stores and activation of Ca^{2+} release-activated Ca^{2+} currents (I_{CRAC}). Here, we report that the ER protein orosomucoid like 3 (ORMDL3), the product of the *ORMDL3* gene associated with several autoimmune and/or inflammatory diseases, negatively modulates I_{CRAC}, SOCE, nuclear factor of activated T cells nuclear translocation and interleukin-2 production. ORMDL3 inhibits the Ca^{2+} influx mechanism at the outer mitochondrial membrane, resulting in a Ca^{2+}-dependent inhibition of I_{CRAC} and reduced SOCE. The effect of ORMDL3 could be mimicked by interventions that decreased mitochondrial Ca^{2+} influx and reverted by buffering of cytosolic Ca^{2+} or activation of mitochondrial Ca^{2+} influx. In conclusion, ORMDL3 modifies key steps in the process of T-lymphocyte activation, providing a functional link between the genetic associations of the *ORMDL3* gene with autoimmune and/or inflammatory diseases.

INTRODUCTION

Calcium homeostasis and activation in many cells rely on a Ca^{2+} signal originated via a mechanism known as store-operated calcium entry (SOCE) (1), which in the case of T lymphocytes is of particular relevance and is triggered following antigen binding to the T-cell receptor and endoplasmic reticulum (ER) Ca^{2+} depletion (2). The major Ca^{2+} sensor in the ER, the stromal interaction molecule 1 (STIM1) (3,4), activates plasma membrane-localized Orai channels (5), ultimately giving rise to what is known as the Ca^{2+} release-activated Ca^{2+} current (I_{CRAC}) (6). Similarly, activation of other immune cells, such as mast cells or dendritic cells, also depends on the influx of Ca^{2+} into the cytosol (reviewed in 7). Ca^{2+} signals generated by Orai channels promote the translocation of several transcription factors to the nucleus, the nuclear factor of activated T cells (NFAT) particularly being relevant to lymphocyte physiology (8). Activation and translocation of NFAT, in turn, trigger the transcription of different genes related to T-cell activation such as interleukin 2 (IL-2) (9,10).

Several proteins have been recently reported to modulate CRAC channel-mediated Ca^{2+} signals at different levels. CRACR2A is a cytosolic protein that stabilizes the STIM–Orai interaction in a Ca^{2+}-dependent manner, thereby enhancing SOCE (11). Two other proteins, Golli (12,13) and stanniocalcin 2 (14), interact with STIM1 reducing SOCE. CRAC channels are also regulated by a negative feedback mechanism known as calcium-dependent inactivation (CDI) due to the accumulation of Ca^{2+} in the immediate vicinity of the channels (15–17). Two proteins have been described to participate in this process. Interaction of calmodulin with both STIM1 and Orai1 triggers rapid CDI of the CRAC channel (18), while the ER protein SARAF associates with STIM to facilitate slow CDI (19).

*To whom correspondence should be addressed at: Laboratory of Molecular Physiology and Channelopathies, Universitat Pompeu Fabra, Parc de Recerca Biomèdica de Barcelona, Room 341, C/Dr Aiguader 88, Barcelona 08003, Spain. Tel: +34 933160854; Fax: +34 933160901; Email: ruben.vicente@upf.edu
†The authors wish it to be known that, in their opinion, the first two authors should be regarded as joint First Authors.

The calcium buffering system of the cell, which includes Ca^{2+} uptake into the ER and mitochondria as well as extrusion via the plasma membrane, also modulates I_{CRAC} current by preventing CDI (20–25). In this context, it is important to point out that ER and mitochondrial shaping of calcium signals may be functionally connected at the mitochondrial-associated membranes (MAMs) (26) which are the zones of close contact between these organelles. Several proteins act as tethering sites at MAMs, including calcium transporters such as the sarco-endoplasmic calcium ATPase pump (SERCA) and inositol trisphosphate receptors in the ER membrane and the voltage-dependent anion channel in the outer mitochondrial membrane (26,27).

The ER-resident transmembrane protein orosomucoid like 3 (ORMDL3) (28) regulates ER calcium homeostasis via inhibition of SERCA2b (29) and modulates the unfolded protein response (29,30). ORMDL3 is coded by the *ORMDL3* gene, whose expression has been reported in the cells that participate in the inflammatory response such as T lymphocytes (28,31). Single nucleotide polymorphisms located in the regulatory regions modify *ORMDL3* expression levels and have been associated with different immune-mediated inflammatory diseases such as asthma, ulcerative colitis, type 1 diabetes and Crohn's disease (30–33). All these diseases also share a deregulation of T-lymphocyte activation (33–36).

Given the findings that (1) ORMDL3 is associated with several inflammatory and autoimmune diseases; (2) ORMDL3 regulates ER Ca^{2+} homeostasis; (3) Ca^{2+} influx is essential for triggering T-lymphocyte activation and (4) T-lymphocyte activation is a key step in the proinflammatory response; we postulate that ORMDL3 expression might be affecting SOCE and T-lymphocyte activation.

RESULTS

ORMDL3 alters cytoplasmic calcium levels and ER Ca^{2+} release in lymphocytes

To elucidate the role of ORMDL3 in lymphocyte physiology and the link between genetic associations of the *ORMDL3* gene with autoimmune and/or inflammatory diseases, we have investigated the impact of ORMDL3 on Ca^{2+} homeostasis and activation of Jurkat T cells.

We first reassessed whether the effect of ORMDL3 overexpression on the cytoplasmic and ER Ca^{2+} levels in Jurkat T cells was similar to what was previously reported for HEK293 cells (29). ORMDL3 overexpression in Jurkat T cells increased cytoplasmic Ca^{2+} (Fig. 1A) and decreased the ER Ca^{2+} release triggered by the SERCA inhibitor cyclopiazonic acid (CPA, 30 μM), which mainly reflects the amount of Ca^{2+} stored in the ER (Fig. 1B and C). Similar results were obtained with the siRNA-mediated knockdown of the SERCA pump (Fig. 1A, D and E), thereby confirming our previous results that proposed the interaction of ORMDL3 with SERCA causing the inhibition of the pump (29). ORMDL3 knockdown with siRNA increased ER Ca^{2+} release (Fig. 1D and E) with no apparent effect on basal cytoplasmic Ca^{2+} (Fig. 1A).

ORMDL3 regulates store-operated calcium entry

Ca^{2+} signaling is of paramount importance in immune system physiology. Indeed, activation of T cells depends on a sustained increase in cytosolic Ca^{2+} concentration through SOCE (7,8). We evaluated SOCE in transiently transfected Jurkat T cells incubated with anti-CD3 antibody and stimulated with a secondary antibody that promotes TCR aggregation and SOCE (Fig. 2). ORMDL3 overexpression reduced Ca^{2+} entry, seen upon addition of Ca^{2+} to the extracellular medium, compared with its control ORMDL3-△1-16 (Fig. 2A and B), an ORMDL3 mutant lacking the cytosolic N-terminal domain. This N-terminal sequence is not present in the yeast orthologs, Orms (Supplementary Material, Fig. S1A and B). When expressed in Jurkat T lymphocytes and HEK293 cells, ORMDL3- △1-16 showed the same characteristics as GFP transfected control cells (Supplementary Material, Fig. S1C and D). Thereafter, this mutant was used as a control in overexpression experiments. On the other hand, siRNA-mediated knockdown of ORMDL3 increased SOCE after CD3 stimulation (Fig. 2C and D).

ORMDL3 modulates Ca^{2+} released-activated Ca^{2+} currents

Ca^{2+} influx following depletion of ER stores occurs through what is classically known as the CRAC channel, formed by the Orai protein (37–39). We analyzed endogenous whole-cell CRAC current (I_{CRAC}) in Jurkat T cells transiently transfected with ORMDL3-WT or ORMDL3-△1-16 (Fig. 3A–C). In order to passively deplete ER stores and activate I_{CRAC}, we included the Ca^{2+} chelator EGTA (10 mM) in the internal pipette solution (6). Our results show that compared with the cells overexpressing ORMDL3- △1-16, the cells overexpressing ORMDL3-WT presented a decrease in current density and a delay in the development of the current (Fig. 3A–C). Downregulation of ORMDL3 expression with siRNA provoked an increase in current density and a faster development of I_{CRAC} compared with control siRNA (Fig. 3D–F).

Yeast ORMDL3 orthologs, Orms, are implicated in sphingolipid metabolism (40,41). Orms inhibit serin palmitoyltranferase (SPT) and block the sphingolipid biosynthetic pathway, although at present it is not known whether a similar function is preserved in mammalian ORMDLs. Myriocin is a specific inhibitor of the SPT that has been previously used as a pharmacological tool to mimic Orms function (40,41). However, treatment with 10 μg/ml myriocin for 24 h did not affect the current density or the delay time of I_{CRAC} (Supplementary Material, Fig. S2).

ORMDL3 modifies lymphocyte activation

A sustained Ca^{2+} concentration increase in the cytoplasm promotes NFAT dephosphorylation and its nuclear translocation (8). We tested NFAT nuclear translocation by confocal microscopy in resting and activated Jurkat T lymphocytes. To monitor NFAT location, we overexpressed a NFAT1–GFP fusion protein and quantified the NFAT1–GFP signal present in the nucleus at 30 and 6 h after activation with

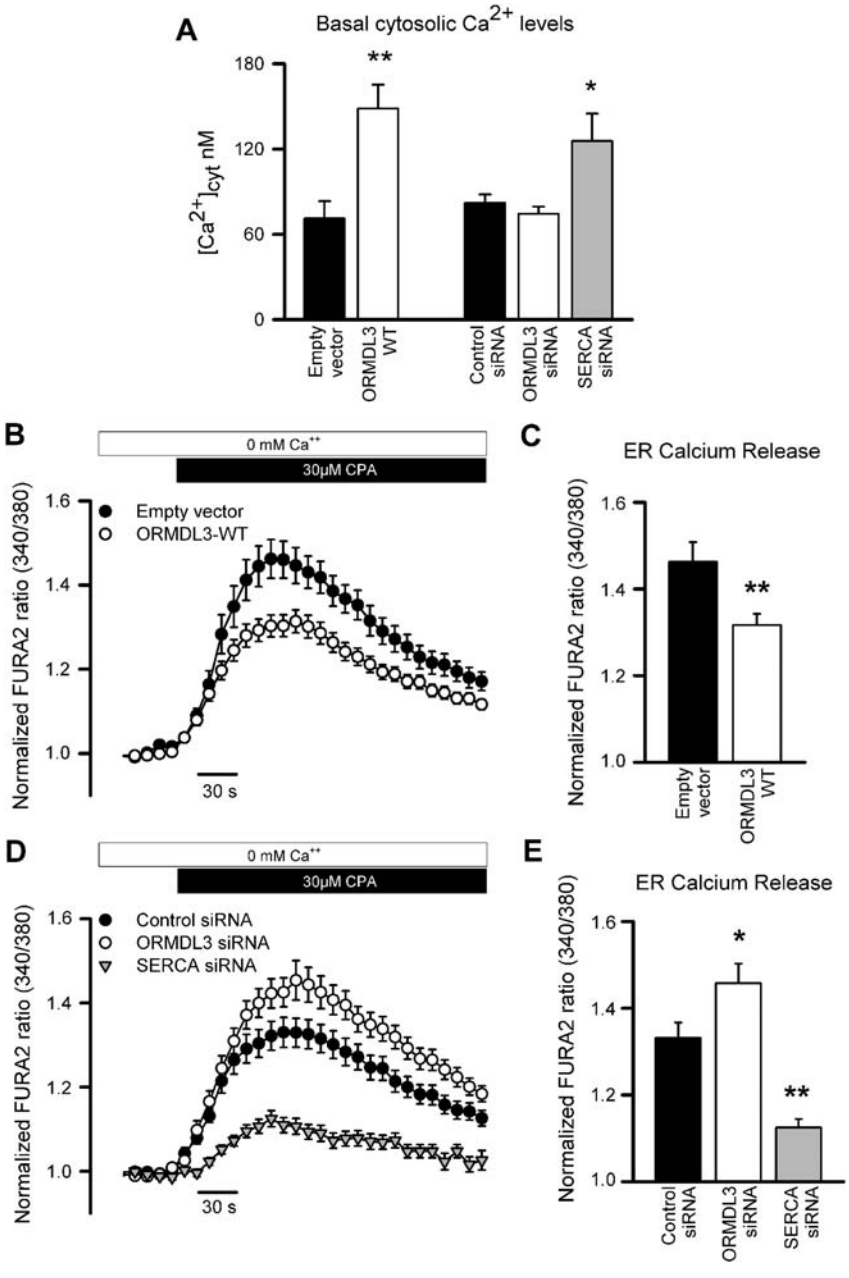

Figure 1. Effect of ORMDL3 on cytosolic calcium levels and ER release in Jurkat T cells. (**A**) Basal cytosolic [Ca^{2+}] in cells transfected with empty vector ($n = 15$), ORMDL3-WT ($n = 25$), control siRNA ($n = 25$), ORMDL3 siRNA ($n = 25$) and SERCA siRNA ($n = 15$). $^{*}P = 0.013$, $^{**}P = 0.002$. (**B–E**) Ca^{2+} signals generated by addition of 30 μM CPA to a Ca^{2+}-free containing solution to promote the passive release of Ca^{2+} from ER. (B) Time course and (C) mean peak values obtained from the cells transfected with ORMDL3-WT ($n = 111$) and empty vector ($n = 92$). $^{**}P = 0.0001$. (D) Time course and (E) the mean peak values from the cells transfected with ORMDL3 siRNA ($n = 76$), control siRNA ($n = 65$) and SERCA siRNA ($N = 49$). $^{*}P = 0.03$, $^{**}P = 0.0001$. Data are presented as mean ± SEM.

thapsigargine (TG, 1 μM) plus phorbol 12-myristate 13-acetate (PMA, 20 nM) (Fig. 4A and B).

Compared with ORMDL3-△1-16, overexpression of ORMDL3-WT reduced the translocation of NFAT to the nucleus in activated cells (Fig. 4A), while siRNA-mediated downregulation of ORMDL3 was associated with higher NFAT translocation 6 h after activation (Fig. 4B). However, no difference in NFAT translocation was observed under these conditions at 30 min. These results are in agreement with previous data showing that reduction of as much as 50% of the SOCE response mainly impacts on the late phase of NFAT translocation (42).

One of the earliest genes transcribed following the activation program in T cells and used as an early marker of activation is IL-2. We tested IL-2-positive cells using a flow cytometry-based intracellular staining technique in Jurkat T cells in which ORMDL3 was overexpressed or downregulated (Fig. 4C and D). The cells were activated as described above

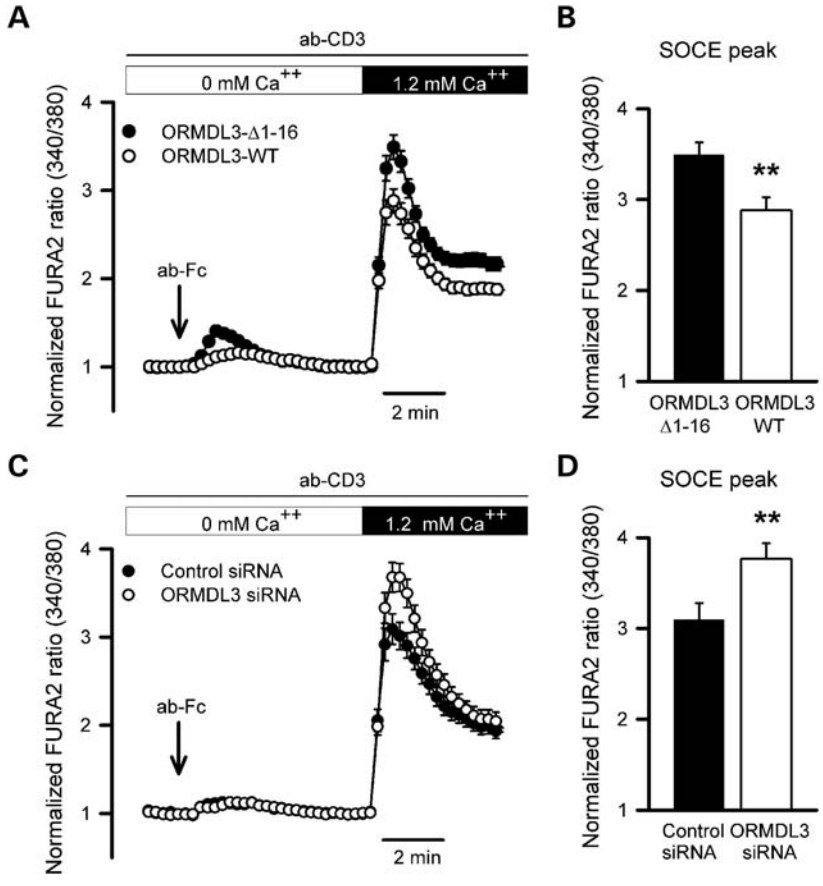

Figure 2. Effect of ORMDL3 on SOCE in Jurkat T cells. Cytosolic Ca^{2+} levels evaluated in the cells preincubated with mouse anti-human CD3. ER Ca^{2+} release triggered by addition of anti-Fc-specific antibody (1:100) to a Ca^{2+}-free solution and SOCE evaluated following readdition of Ca^{2+} to the bathing solution. (**A** and **B**) Time course and mean peak values obtained from the cells transfected with ORMDL3-WT ($n = 67$) and ORMDL3-Δ1-16 ($n = 60$). $^{**}P = 0.0026$. (**C**) Time course and (**D**) mean peak values obtained from the cells transfected with ORMDL3 siRNA ($n = 54$) and control siRNA ($n = 43$). $^{**}P = 0.01$. Data are presented as mean ± SEM.

and 6 h after activation a population of cells producing IL-2 showed up. This population was reduced in the cells overexpressing ORMDL3-WT compared with the cells overexpressing ORMDL3-Δ1-16 (Fig. 4C). Downregulation of ORMDL3 expression with siRNA resulted in an increased population of cells producing IL-2 (Fig. 4D).

ORMDL3 localizes near STIM–Orai puncta

The trigger for the opening of CRAC channels involves the interaction between STIM proteins located in the ER and Orai proteins present in the plasma membrane (43). We analyzed whether ORMDL3 colocalized with STIM1 and Orai1. A line scan of confocal images of cells overexpressing Orai1-YFP, STIM1-CFP and either ORMDL3-WT or ORMDL3-Δ1-16 showed that both ORMDLs colocalized with STIM1 in unstimulated cells and moved with STIM1 towards the plasma membrane puncta upon activation of Jurkat T cells (Supplementary Material, Fig. S3). However, we ruled out the possibility that ORMDL3 interacts directly with STIM as no coimmunoprecipitation was detected between ORMDL3 and this protein (Supplementary Material, Fig. S4). Similar colocalization results were obtained for the ORMDL3-Δ1-16 mutant, thereby discarding misslocalization of the mutant ORMDL3 as the reason for its lack of function. Besides, the differences in I_{CRAC} and SOCE observed following alteration of ORMDL3 expression levels were not due to differences in the expression of STIM1 or Orai1, which remained unmodified (Supplementary Material, Fig. S4).

ORMDL3 increases I_{CRAC} calcium-dependent inactivation

CRAC channel activity is negatively regulated by cytosolic Ca^{2+} levels in both a fast and slow time scale (15–17), a process that is prevented with strong buffering of the intracellular Ca^{2+}. In order to explore whether the mechanism behind ORMDL3 modulation of SOCE was related to CDI of CRAC channels, we recorded endogenous whole-cell I_{CRAC} using the fast Ca^{2+} chelator BAPTA (as slow CDI is not fully prevented in the presence of 10 mM EGTA (44,45)) in the internal solution of the patch pipette. In the presence of BAPTA, ORMDL3 overexpression did not produce any effect on I_{CRAC} development or the current density (Fig. 5A and B). This result suggested that ORMDL3 affects I_{CRAC} CDI. To further explore

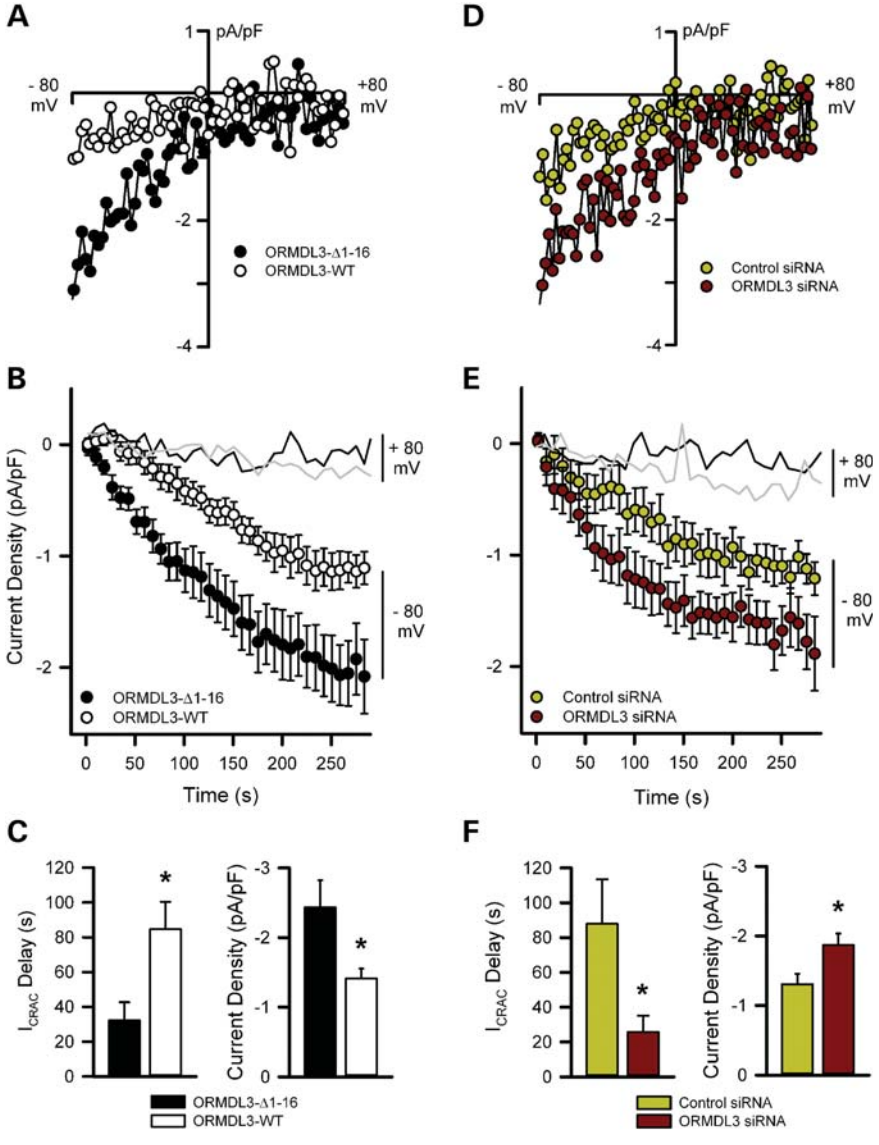

Figure 3. ORMDL3 expression modifies endogenous I_{CRAC} currents in Jurkat T cells. (**A**) I_{CRAC} current–voltage ramps recorded from Jurkat T cells overexpressing ORMDL3-Δ1-16 or ORMDL3-WT at t = s. (**B**), Time course of the current density recorded at −80 mV (symbols) and +80 mV (lines) in Jurkat cells overexpressing ORMDL3-Δ1-16 (black) and ORMDL3-WT (white, grey). (**C**) Time constant of I_{CRAC} development (left) and mean peak current density recorded at −80mV (right) in Jurkat cells overexpressing ORMDL3-Δ1-16 and ORMDL3-WT current delay $^{*}P = 0.01$ and current density $^{*}P = 0.02$. (**D**) I_{CRAC} current–voltage ramps recorded from Jurkat T cells transfected with control siRNA or ORMDL3 siRNA. (**E**) Time course of current density recorded at −80 mV (symbols) and +80 mV (lines) in Jurkat cells transfected with control siRNA (black) or ORMDL3 siRNA (white,grey). (**F**) Time constant of I_{CRAC} development (left) and mean peak current density recorded at −80mV (right) in Jurkat cells transfected with control siRNA or ORMDL3 siRNA. Current delay $^{*}P = 0.04$ and current density $^{*}P = 0.02$. ORMDL3-Δ1-16 ($n = 13$); ORMDL3-WT ($n = 13$); control siRNA ($n = 10$); ORMDL3 siRNA ($n = 10$). Data are presented as mean ± SEM.

whether ORMDL3 affects slow CDI, the cells were incubated in Ca^{2+}-free solutions containing TG (1 μM) and recorded with weak intracellular Ca^{2+} buffering. Upon addition of Ca^{2+} to the bath solution, I_{CRAC} developed (represented as percentage of the maximal current), showing a faster rundown in ORMDL3-WT transfected cells compared with ORMDL3-△1-16 expressing cells (Fig. 5C and E). An addition of high concentrations of the slow Ca^{2+} chelator EGTA (20 mM) to the pipette solution abolished the ORMDL3-induced slow CDI of I_{CRAC} (Fig. 5D and F). Together these experiments suggested an ORMDL3-dependent modulation of I_{CRAC} CDI.

ORMDL3 binds to and inhibits the SERCA pump promoting cytosolic calcium accumulation (29), although several pieces of evidence argue against the ORMDL3-dependent inhibition of SERCA as the cause of the increased I_{CRAC} CDI observed in the cells overexpressing ORMDL3. First, the ORMDL3-dependent effect on I_{CRAC} slow CDI appeared in the presence of the irreversible SERCA inhibitor TG (Fig. 5C). Second, we obtained a similar reduction in SOCE response when we applied CPA (Supplementary Material, Fig. S5A) or anti-CD3 (Fig. 2A). Third, siRNA-mediated knockdown of SERCA reduced the CPA-induced ER Ca^{2+} release but did not affect SOCE (Supplementary Material,

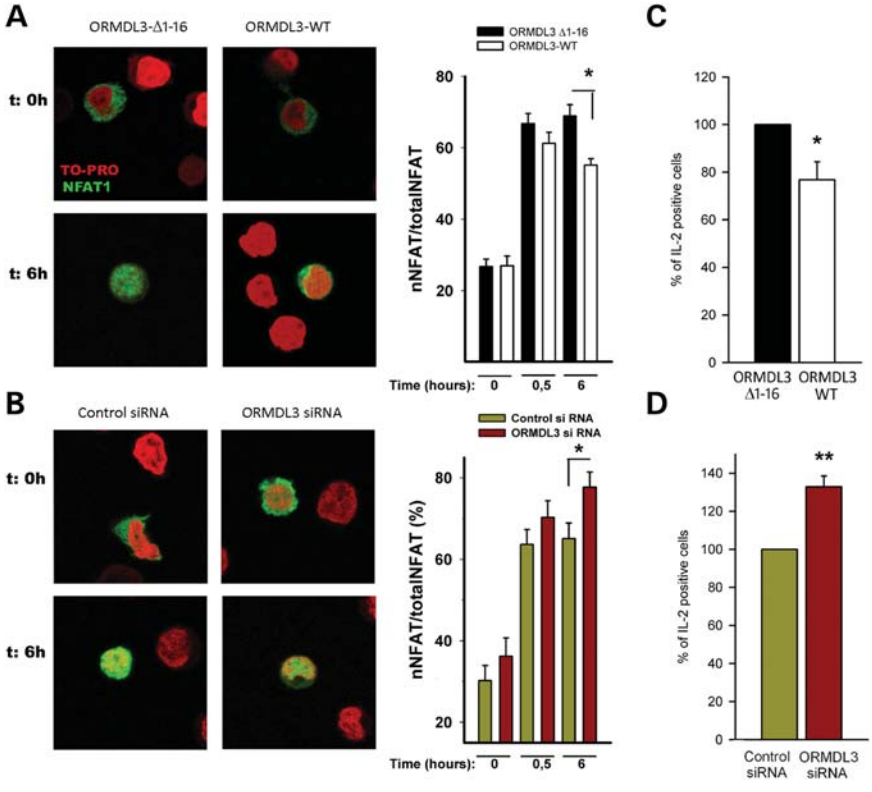

Figure 4. ORMDL3 modulates nuclear NFAT1 translocation. (**A** and **B**) Representative images showing NFAT1-GFP (green) and TO-PRO (red) for every transfection condition at basal and 6 h after activation with PMA (20 nM) and thapsigargine (TG, 1 μM). The quantification of NFAT1 present in the nucleus was obtained dividing the nuclear signal of NFAT-GFP (colocalizing with TO-PRO) by the total NFAT1-GFP signal for each cell. (**A**) (right) mean values of nuclear NFAT1 present at basal, 30 min and 6 h in cells overexpressing ORMDL3-Δ1-16 ($n = 39$) or ORMDL3-WT ($n = 103$). $^*P = 0.0001$. (**B**) (right) mean values of nuclear NFAT1 present at basal, 30 min and 6 h in cells overexpressing control siRNA ($n = 17$) or ORMDL3 siRNA ($n = 17$). $^*P = 0.02$. (**C** and **D**) Jurkat T cells were cotransfected with GFP and ORMDL3-Δ1-16, ORMDL3-WT, control siRNA or ORMDL3 siRNA. 24 h after transfection cells were activated with PMA (20 nM) and TG (1 μM) for 6 h and stained using an IL-2 antibody. A minimum of 3000 GFP-positive cells were taken for each experiment. (C) Mean percentage of IL-2-positive cells under ORMDL3-WT conditions referred to ORMDL3-Δ1-16 ($n = 3$). $^*P = 0.03$. (D) Mean percentage of IL-2-positive cells under ORMDL3 siRNA conditions referred to control siRNA ($n = 6$). $^*P = 0.0002$. Data are presented as mean ± SEM.

Fig. S5B). Altogether, these results suggested the participation of a mechanism different from the ORMDL3-mediated inhibition of SERCA in the ORMDL3-mediated modulation of SOCE in Jurkat T cells.

ORMDL3 reduces mitochondrial calcium uptake

In an attempt to identify the mechanism of ORMDL3-dependent modulation of SOCE, we focused our attention on mitochondria as Ca^{2+} influx into these organelles modulates I_{CRAC} CDI and SOCE (23,24,46).

Punctual colocalization of ORMDL3 with mitotracker was detected in Jurkat cells (Supplementary Material, Fig. S6A), which was similar to that described for ER proteins present at the ER–mitochondria junctions (27). Application of antimycin A and oligomycin (which both depolarize mitochondrial potential and thereby impair Ca^{2+} uptake into the mitochondria (47)) reduced SOCE in ORMDL3-Δ1-16 expressing cells to the level seen in ORMDL3-WT expressing cells (Fig. 6A, left). On the other hand, kaempferol, an activator of the mitochondrial Ca^{2+} uniporter (48), reverted the ORMDL3-induced SOCE phenotype back to control (ORMDL3-Δ1-16) levels (Fig. 6A, middle). Together, these experiments showed that the effect of ORMDL3 overexpression on SOCE was mimicked by pharmacological manipulation of mitochondrial Ca^{2+} influx (Fig. 6A right). Next, we evaluated whether ORMDL3 could affect Ca^{2+} influx into the mitochondria using a mitochondrially targeted GFP-based ratiometric Pericam Ca^{2+} sensor (mtPericamR) (49) and the low Ca^{2+} affinity dye rhod-5N (50).

We evaluated mitochondrial Ca^{2+} uptake in permeabilized Jurkat T cells expressing mtPericamR and ORMDL3-WT or ORMDL3-Δ1-16 exposed to identical $[Ca^{2+}]_{cyt}$. Following the permeabilization of the plasma membrane with digitonin under Ca^{2+}-free conditions, Ca^{2+} was added to the external solution to trigger mitochondrial Ca^{2+} influx. Under these conditions, Ca^{2+} influx into the mitochondria of ORMDL3-expressing cells was lower than in ORMDL3-Δ1-16 expressing cells (Fig. 6B), pointing to a deficient mitochondrial Ca^{2+} influx as the primary cause of increased I_{CRAC} CDI and reduced SOCE. Opposite results of mitochondrial uptake were obtained downregulating ORMDL3 with siRNAs (Fig. 6C). Similar changes in mitochondrial $[Ca^{2+}]$ were obtained using CPA in non-permeabilized cells or using the calcium dye rhod-5N (Supplementary Material, Fig. S6).

Finally, considering that removal of the N-terminus renders ORMDL3 unable to regulate SOCE, we tested the effect of

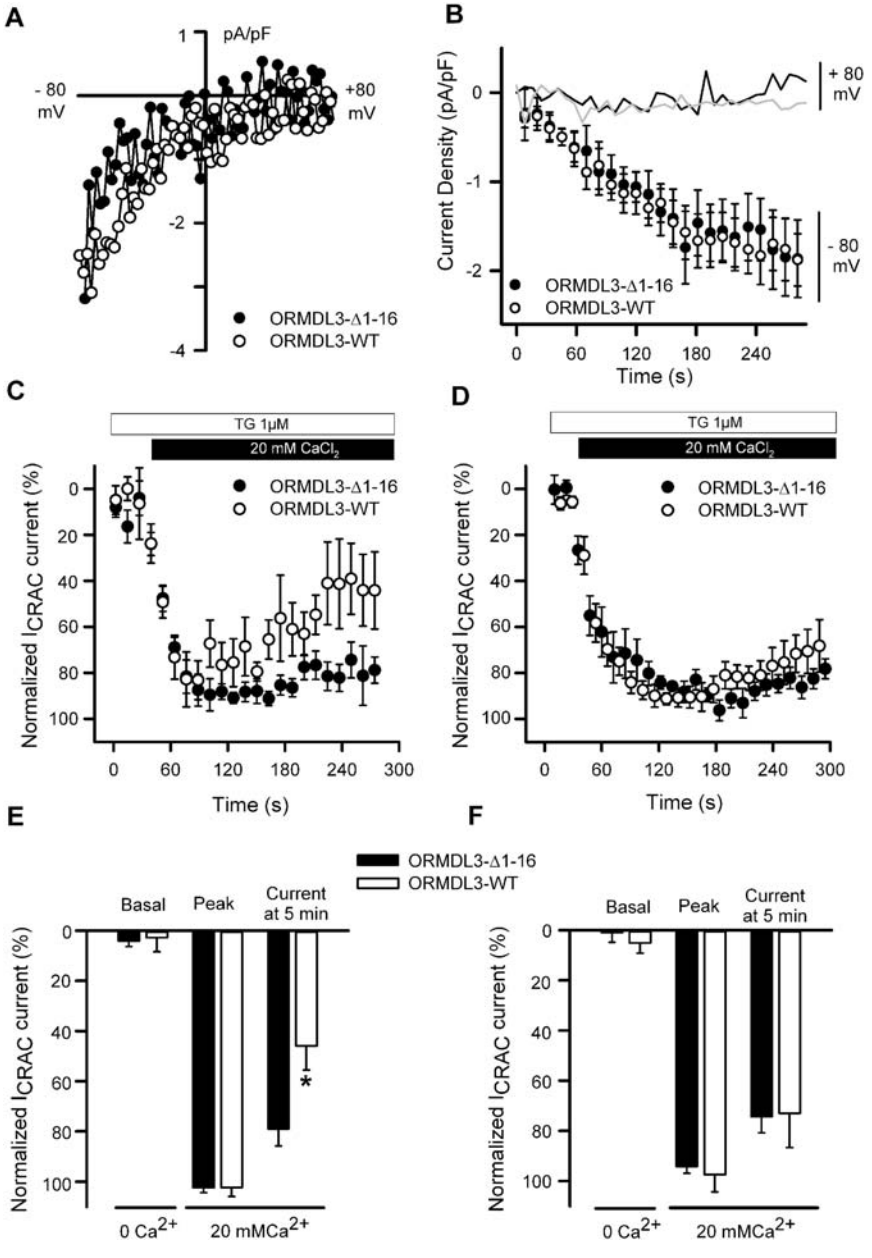

Figure 5. ORMDL3 increases I_{CRAC} CDI: (**A**) I_{CRAC} current–voltage ramps recorded from Jurkat T cells overexpressing ORMDL3-Δ1-16 or ORMDL3-WT at t = 283 s in the presence of 10 mM BAPTA in the pipette. (**B**) Time course of current density recorded at −80 mV (symbols) and +80 mV (lines) in Jurkat T cells dialyzed with BAPTA and overexpressing ORMDL3-Δ1-16 (black, $n = 5$) or ORMDL3-WT (white, grey; $n = 6$). (**C**) Time course of normalized current ($I_{CRAC}/I_{CRACmax}$) recorded at −100 mV in Jurkat T cells dialyzed with 1.2 mM EGTA after depletion of intracellular stores with TG and addition of 20 mM Ca^{2+} to the bathing solution (ORMDL3-Δ1-16, $n = 7$; and ORMDL3-WT, $n = 6$). (**D**) Normalized mean currents recorded as in (C) but using pipette solutions containing 20 mM EGTA (ORMDL3-Δ1-16, $n = 7$; and ORMDL3-WT, $n = 6$) (**E**) Mean normalized current measured at three different times (from C): in the absence of calcium (left), peak (middle) and current remaining at 5 min (right) following the addition of Ca^{2+}. (**F**) Mean normalized current measured at three different times (from D): in the absence of calcium (left), peak (middle) and current remaining at 5 min (right) following the addition of Ca^{2+}. $^{*}P = 0.01$. Data are presented as mean ± SEM.

the N-terminus isolated from the rest of the protein. Overexpression of amino acids 1–20 of ORMDL3 mimicked the effect of the whole ORMDL3 protein on SOCE and mitochondrial Ca^{2+} influx (Fig. 6D and E). Altogether, our results indicated that ORMDL3 affects mitochondrial Ca^{2+} influx and the Ca^{2+} buffering capacity of the cell, thereby affecting the CDI of CRAC channels.

DISCUSSION

The association of the *ORMDL3* gene with several proinflammatory and autoimmune diseases suggests that ORMDL3 protein may play an important role in the immune system physiology. Cells of the immune system express *ORMDL3* (28,31) and increased expression of *ORMDL3* has been

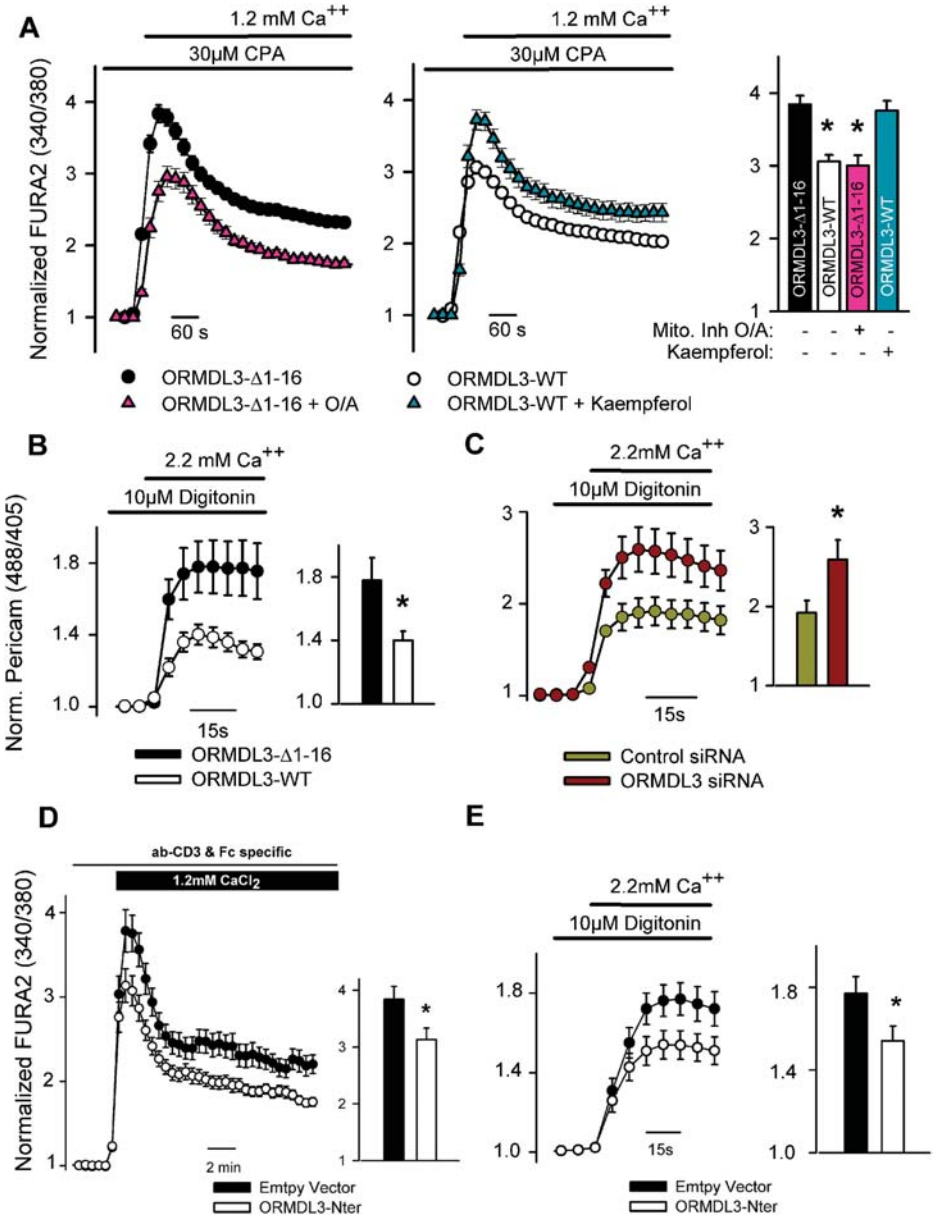

Figure 6. ORMDL3 affects mitochondrial buffering capability. Left, SOCE in cells transfected with ORMDL3-△1-16 in the presence or absence of oligomycin and antimycin (**A**) (O/A) to depolarize the mitochondria. Middle, SOCE in cells transfected with ORMDL3-WT in the presence ($n = 50$) or absence ($n = 75$) of kampferol, an activator of the mitocondria Ca^{2+} uniporter. Right, mean peak responses. $^*P = 0.0001$. (**B** and **C**) Mitochondrial Ca^{2+} signal measured using the mtPericam sensor after readdition of extracellular Ca^{2+} to Jurkat cells overexpressing ORMDL3-Δ1-16 ($n = 25$) or ORMDL3-WT ($n = 18$, $^*P = 0.04$); or exposed to ORMDL3 siRNA ($n = 27$) and control siRNA ($n = 40$; $^*P = 0.01$). Cells were pretreated with 10 μM digitonin in a free calcium external solution (**D**) SOCE elicited by anti-human CD3 preincubated Jurkat T cells was carried out as described in Fig. 2. Expression of ORMDL3-Nter ($n = 48$) decreased SOCE compared with empty vector ($n = 38$; $^*P = 0.02$). (**E**) Mitochondrial calcium uptake using a mtPericam sensor in Jurkat cells expressing either ORMDL3-Nter ($n = 58$) or an empty vector ($n = 57$; $^*P = 0.03$). Data are presented as mean ± SEM.

associated with higher risk of childhood asthma (31). We have previously shown that the product of this gene is an ER protein that participates in ER-mediated Ca^{2+} homeostasis and stress responses (29), thereby providing a link between asthma, ORMDL3 and dysregulation of Ca^{2+} homeostasis. Additional support for the hypothesis that genetic variants with impact in Ca^{2+} homeostasis are relevant to asthma pathophysiology comes from an association study of transient receptor potential cationic channels with the severity of childhood asthma (51)(reviewed by 52). In the present study, we have carried out a deeper evaluation of ORMDL3 function focusing on the impact of ORMDL3 on SOCE and lymphocyte activation. Our results show that ORMDL3 modulates SOCE and lymphocyte activation, an effect that may sum to the previously described effect on ER Ca^{2+} imbalance and stress (29).

We have shown that overexpression of ORMDL3 decreases SOCE and T-cell activation. Impaired Ca^{2+} signaling in T cells has been linked to inherited immunodeficiency diseases

(37) but evidences also exist linking deficient T-cell Ca^{2+} signaling to proinflammatory conditions. Mice lacking both STIM1 and STIM2 present an impaired SOCE but show splenomegaly, lymphadenopathy and leukocyte infiltration in several tissues, including lungs, due to anomalous regulatory T-lymphocyte development (42,53). Similarly, ablation of the signaling cascade downstream SOCE (e.g. NFAT (54)) or mutations in the upstream signaling elements (in the linker for activation of T cells (LAT) that prevent PLCγ activation (55,56)) resulted in mice presenting lymphoproliferative and autoimmune phenotypes. In summary, it is possible that disruption of the fine tuning of the SOCE-NFAT pathway determines T-cell dysfunction, which may be expressed at the individual level as proinflammatory or immunodeficient conditions. It is not yet known how ORMDL3 may be affecting the immune system in animal models but the fact that it modulates lymphocyte activation suggests that it may also have an impact on the overall immune system response.

Our results demonstrate that ORMDL3 modifies SOCE response by altering the slow CDI of the CRAC channel, an effect that requires the N-terminus of the protein, which is sufficient to induce modulation of the SOCE. ORMDL3 binds to and inhibits the SERCA pump (29) reducing the ER calcium content. Both, SERCA (21) and ORMDL3 (this study), localize close to the STIM-Orai interaction sites in activated lymphocytes. However, ORMDL3-mediated modulation of I_{CRAC} and SOCE is independent of SERCA activity since these effects are observed in the presence of SERCA inhibitors.

In our search for factors that may explain the ORMDL3-mediated differences in I_{CRAC} and SOCE, we focused on the mitochondria as these organelles are found in close proximity to both the ER and the plasma membrane (26,57) and are capable of modulating Ca^{2+} signals (58,59). Through their ability to take up cytoplasmic Ca^{2+}, mitochondria exert a dual effect on SOCE. Mitochondrial competition for the Ca^{2+} used by SERCA to refill the ER initially enhances I_{CRAC} activation (accelerating I_{CRAC} development), while in a slower time scale reduces inactivation of CRAC channels (23,46,60,61). Besides that, mitochondria migrate near Orai channels during SOCE activation and formation of an immunological synapse, further favoring the removal of calcium from the channel vicinity and preventing CDI (62,63). Mitochondria has also been recently proposed to exert a permissive role in STIM1 trafficking (64).

The fact that mitochondrial Ca^{2+} uptake is impaired in ORMDL3 overexpressing cells and enhanced by knocking down ORMDL3 with siRNA may explain the effect of ORMDL3 on I_{CRAC} and SOCE. Several pieces of evidence support this conclusion. First, depolarization of the mitochondrial potential, preventing mitochondrial calcium buffering capacity, mimics the ORMDL3 effect on SOCE, while favoring mitochondrial Ca^{2+} import upon application of kaempferol reverts the effect of ORMDL3 on SOCE. Second, the changes in I_{CRAC} development vary according to a reduced mitochondrial Ca^{2+} influx (increased delay in ORMDL3 overexpressing cells) or increased mitochondrial Ca^{2+} influx (reduced delay in ORMDL3 siRNA-treated cells). Third, augmented I_{CRAC} CDI in ORMDL3 expressing cells is also consistent with a reduced mitochondrial Ca^{2+} influx. The fact that high concentration of EGTA (and lower concentration of BAPTA) reduced the ORMDL3-induced CDI of I_{CRAC} along with the involvement of the mitochondria in this process suggests that ORMDL3 affects I_{CRAC} slow CDI. Fourth, the ORMDL3-mediated changes in mitochondrial Ca^{2+} influx are not secondary to alterations in SOCE as similar changes were obtained in permeabilized cells exposed to the same $[Ca^{2+}]$. Fifth, we observed punctual colocalization of ORMDL3 with mitochondria, similar to that described for the physical interacting spots between ER and mitochondria called MAMs (26). We have not evaluated whether ORMDL3 may be also affecting the metabolic activity and the ATP production at the mitochondria, which in turn may be affecting the SERCA pump activity and ER calcium refilling (65).

Yeast orthologs of *ORMDL3* (*Orms*) participate in sphingolipid metabolism and stress pathways (40,41). However, in our hands myriocin did not affect I_{CRAC} in Jurkat T cells. Moreover, the N-terminus region of Orms, essential for its activity regulation (66–68), is not conserved in mammals. Nevertheless, our experiments with the ORMDL3-Δ1-16 mutant and the overexpression of the N-terminus alone demonstrate that the residues present in the mammalian N-terminus are essential for the ORMDL3 activity.

In conclusion, we have shown that ORMDL3 expression levels modify T-cell calcium signaling and lymphocyte activation following the alteration of the mitochondrial Ca^{2+} influx and I_{CRAC} CDI. Our data point to ORMDL3 as the first ER-based protein modulating Ca^{2+} transport into the mitochondria and places it at an important position in the control of Ca^{2+} transport into the major intracellular stores. Moreover, our data offer a pathophysiological mechanism, the regulation of SOCE and lymphocyte activation, by which ORMDL3 may be participating in those immune and/or inflammatory diseases showing altered levels of *ORMDL3* expression.

MATERIALS AND METHODS

Reagents, plasmids and cell culture

Jurkat T cells were maintained in Roswell Park Memorial Institute medium plus 10% fetal bovine serum (FBS) and HEK293 cells were cultured in Dulbecco's modified Eagle's medium plus 10% FBS. Transient transfection of Jurkat T cells and HEK293 cells was carried out using TransIT-Jurkat transfection reagent (Mirus Bio Corporation) and ExGen500 (Fermentas MBI), respectively.

Activation of Jurkat T cells was carried out with phorbol-12-myristate-13-acetate (PMA, 20 nM) and TG (1 μM) for 6 h. For those experiments using myriocin (10 μg/ml) to inhibit the serine palmitoyltranferase enzyme, the cells were treated for 24 h. All chemicals unless otherwise indicated were obtained from Sigma.

ORMDL3 amino terminal deletion (ORMDL3-Δ1-16) was generated by PCR and cloned into pCDNA3 vector. The sequence of the ORMDL3 N-terminus was cloned in a pcmv-myc expressing vector (ORMDL3-Nter) producing the following fusion peptide MASMQKLISEEDLLMAMEARILNVGTAHSEVNPNTRVMNSR. NFAT1 expression vector was a kind gift from Dr J. Aramburu (Universitat Pompeu Fabra), pmaxSTIM1-CFP and pmaxOrai1-YFP were a gentle gift from Dr Samelson LE (National Cancer Institute,

Bethesda). All constructs were verified by sequencing (Big Dye 3.1, AbiPrism, Applied Biosystems).

ORMDL3 siRNA (5′-TAAGTACGACCAGATCCATTT-3′) (Qiagen) or control siRNA (5′-AATTCTCCGAACGTGTCACGT-3′) (Qiagen) was used in the expression knockdown experiments (29). SERCA siRNA was purchased from Invitrogen. These siRNAs were transfected using Lipofectamin 2000 (Invitrogen).

Measurement of intracellular [Ca^{2+}]

A cytosolic Ca^{2+} signal was determined in cells loaded with 4.5 μM fura-2·AM (20 min) as previously described (69). Cytosolic [Ca^{2+}] increases are presented as the ratio of emitted fluorescence (510 nm) after excitation at 340 and 380 nm, relative to the ratio measured prior to cell stimulation (fura-2 ratio 340/380).

Mitochondrial calcium levels were obtained in cells loaded for 15 min at 37°C with 5 μM rhodamine-5N-AM (50) or transfected with mtPericamR (49). Calcium increases in rhodamine-loaded cells are presented as an increase in emitted fluorescence (590 nm) after excitation (561 nm). Ratiometric-pericam-mt imaging was obtained by excitation at 410 and 488 nm and emission at 520 nm in a Leica TCS SP5 confocal microscope with a 40× Oil objective and analyzed using ImageJ software. All experiments were carried out at room temperature and the cells were bathed in a solution containing (in mM): 140 NaCl, 5 KCl, 1.2 $CaCl_2$, 0.5 $MgCl_2$, 5 glucose, 10 HEPES; 300 mosmol/l, pH 7.4 with Tris). Ca^{2+}-free solutions were obtained by replacing $CaCl_2$ with equal amounts of $MgCl_2$ plus 0.5 mM EGTA and 10 μM Digitonin when indicated.

Store depletion was achieved in Jurkat T cells using anti-CD3 hybridoma SN and crosslinked with a secondary anti-Fc-specific mouse antibody (Sigma m2650 1:100). CPA was used at 30 μM and 10 μM in Jurkat and HEK293 cells, respectively.

NFAT nuclear translocation assay and immunostaining

Cells were transfected with NFAT1-GFP plus ORMDL3, ORMDL3-Δ1-16 or with siRNAs. After transfection, the cells were seeded on poly-L-lysine pretreated coverslips at the indicated time lapses. The cells were fixed with 4% paraformaldehyde for 15 min and nuclear staining was performed for 10 min with TO-PRO3. NFAT translocation was calculated as the ratio of nuclear NFAT-GFP signal to total NFAT1-GFP.

Colocalization experiments were performed in the cells transfected with STIM-CFP and Orai-YFP. After fixation, immunostaining for ORMDL3 was done using a commercial anti-ORMDL3 antibody (1:100, Abgent). Briefly, the cells were permeabilized for 10 min with 0.1% Triton in phosphate buffered saline (PBS). Blocking and antibody incubating solution contained 2% FBS, 1% BSA and 0.5% Triton in PBS. Images were acquired using an inverted Leica SP2 confocal microscope with a 40× 1.32 Oil Ph3 CS objective and analyzed using ImageJ software.

IL2 intracellular staining

Cells transfected with ORMDL3-WT, ORMDL3-Δ1-16 or siRNAs plus GFP were washed twice with ice-cold PBS solution and fixed with paraformaldehyde at 4%. The cells were then permeabilized and blocked with 2% BSA plus 0.5% saponin (in PBS). Intracellular IL-2 staining was carried out using PE rat anti-human IL-2 (BD Pharmagen). LSRII (Beckton Dickinson) 488 laser was used to gate transfected cells and 575/25 filter to evaluate IL2 (PE)-positive cells.

Electrophysiology

Patch-clamp experiments were performed in the whole-cell configuration with fire-polished patch pipettes (3 to 4 MΩ). Pipette and cell capacitance were electronically compensated before each voltage ramp with an EPC-10 patch-clamp amplifier controlled by Patchmaster software (HEKA). Membrane currents were filtered at 2.9 kHz and digitized at a sampling rate of 10 kHz. Whole-cell currents were elicited by 50 ms voltage ramps from −100 (−120 in CDI experiments) to +100 mV from a holding potential of 0 mV. All currents were normalized by cell capacitance. For leak current correction, the ramp current before CRAC activation was subtracted. No differences ($P > 0.05$) in the mean cell capacitance were recorded on cells used under different experimental conditions: ORMDL3 4.9 ± 0.2 pF; ORMDL3-ΔN 4.8 ± 0.2 pF; empty vector 4.4 ± 0.3 pF; siControl 5.5 ± 0.2 pF; siORMDL3 5.5 ± 0.3 pF; DMSO 5.3 ± 0.6 pF; myriocin 4.9 ± 0.6 pF. Mean ± SEM, $n = 5–13$.

Two methods were used to trigger I_{CRAC}. Passive depletion with pipettes filled with a solution containing (in mM): 140 cesium aspartate, 10 NaCl, 5 $MgCl_2$, 10 EGTA (replaced by BAPTA in BAPTA experiment) and 10 HEPES (pH 7.2 with CsOH). The external solution contained (in mM): 155 NaCl, 4.5 KCl, 10 $CaCl_2$, 2 $MgCl_2$, 10 glucose, and 5 HEPES (pH 7.4 with NaOH). For CDI, pipette internal solution contained (in mM): 140 cesium aspartate, 2 $MgCl_2$, 0.66 $CaCl_2$, 1.2 EGTA, 10 HEPES (pH 7.2 with CsOH). To evaluate CDI of I_{CRAC}, the cells were seeded in 0 Ca^{2+} external solution containing (in mM): 135 NaCl, 4.5 KCl, 3 $MgCl_2$, 0.5 EGTA, 10 glucose, 5 HEPES (pH 7.4 with NaOH). After obtaining the whole-cell configuration, the cells were incubated for 3 min in 0 Ca^{2+} external solution + 1 μM TG to completely deplete internal calcium stores and then switch to a solution containing 20 mM Ca^{2+}. All experiments were carried out at room temperature. The calculation of I_{CRAC} delay was carried out using the plateau function followed by one phase association of the Graph Pad Prism 5 software.

Statistics

All data were expressed as means ± SEM. Statistical analysis was performed using Student's *t*-test or one-way analysis of variance using SigmaPlot or OriginPro software. Bonferroni's test was used for *post-hoc* comparison of the mean values. The criterion for a significant difference was a final value of $P < 0.05$.

SUPPLEMENTARY MATERIAL

Supplementary Material is available at *HMG* online.

AUTHORS' CONTRIBUTIONS

M.A.V. is the recipient of an ICREA Academia Award. A.C-S., G.C-R., F.R-M., K.K. and R.V. performed research; A.C-S., G.C-R., F.R-M., C.P., B.A. N., M.A.V. and R.V. analyzed data; A.C-S., G.C-R., M.A.V. and R.V. conceived the core hypothesis and wrote the manuscript. All authors participated in manuscript editing.

ACKNOWLEDGEMENTS

We thank Dr J. Aramburu (University Pompeu Fabra, Spain) for the gift of NFAT-EGFP, Dr LE Samelson (National Cancer Institute, Bethesda, USA) for the gift of pmaxSTIM1-CFP and pmaxOrai1-YFP, C. Plata for the technical support and C. Fandos for his help with the generation of some plasmids. We also thank Professor Markus Hoth (University of Saarland, Germany) for critical reading of the manuscript.

Conflict of Interest statement. None declared.

FUNDING

This work was supported by Spanish Ministry of Science and Innovation (SAF2009-09848; SAF2010-16725, SAF2012-38140), Fondo de Investigación Sanitaria (Red HERACLES RD12/0042/0014), FEDER Funds; Generalitat de Catalunya (SGR05-266) and Fundació la Marató de TV3 (080430). M.A.V. is the recipient of an ICREA Academia Award. A.C-S., G.C-R., F.R-M., K.K. and R.V. performed research; A.C-S., G.C-R., F.R-M., C.P., B.A. N., M.A.V. and R.V. analyzed data; A.C-S., G.C-R., M.A.V. and R.V. conceived the core hypothesis and wrote the manuscript. All authors participated in manuscript editing.

REFERENCES

1. Hogan, P.G., Lewis, R.S. and Rao, A. (2010) Molecular basis of calcium signaling in lymphocytes: STIM and ORAI. *Annu. Rev. Immunol.*, **28**, 491–533.
2. Vig, M. and Kinet, J.P. (2009) Calcium signaling in immune cells. *Nat. Immunol.*, **10**, 21–27.
3. Zhang, S.L., Yu, Y., Roos, J., Kozak, J.A., Deerinck, T.J., Ellisman, M.H., Stauderman, K.A. and Cahalan, M.D. (2005) STIM1 is a Ca^{2+} sensor that activates CRAC channels and migrates from the Ca^{2+} store to the plasma membrane. *Nature*, **437**, 902–905.
4. Liou, J., Kim, M.L., Heo, W.D., Jones, J.T., Myers, J.W., Ferrell, J.E. Jr and Meyer, T. (2005) STIM is a Ca^{2+} sensor essential for Ca^{2+}-store-depletion-triggered Ca^{2+} influx. *Curr. Biol.*, **15**, 1235–1241.
5. Luik, R.M., Wang, B., Prakriya, M., Wu, M.M. and Lewis, R.S. (2008) Oligomerization of STIM1 couples ER calcium depletion to CRAC channel activation. *Nature*, **454**, 538–542.
6. Hoth, M. and Penner, R. (1992) Depletion of intracellular calcium stores activates a calcium current in mast cells. *Nature*, **355**, 353–356.
7. Feske, S. (2007) Calcium signalling in lymphocyte activation and disease. *Nat. Rev. Immunol.*, **7**, 690–702.
8. Gwack, Y., Feske, S., Srikanth, S., Hogan, P.G. and Rao, A. (2007) Signalling to transcription: store-operated Ca^{2+} entry and NFAT activation in lymphocytes. *Cell Calcium*, **42**, 145–156.
9. Shaw, J.P., Utz, P.J., Durand, D.B., Toole, J.J., Emmel, E.A. and Crabtree, G.R. (1988) Identification of a putative regulator of early T cell activation genes. *Science*, **241**, 202–205.
10. Macian, F. (2005) NFAT proteins: key regulators of T-cell development and function. *Nat. Rev. Immunol.*, **5**, 472–484.
11. Srikanth, S., Jung, H.J., Kim, K.D., Souda, P., Whitelegge, J. and Gwack, Y. (2010) A novel EF-hand protein, CRACR2A, is a cytosolic Ca^{2+} sensor that stabilizes CRAC channels in T cells. *Nat. Cell Biol.*, **12**, 436–446.
12. Feng, J.M., Hu, Y.K., Xie, L.H., Colwell, C.S., Shao, X.M., Sun, X.P., Chen, B., Tang, H. and Campagnoni, A.T. (2006) Golli protein negatively regulates store depletion-induced calcium influx in T cells. *Immunity*, **24**, 717–727.
13. Walsh, C.M., Doherty, M.K., Tepikin, A.V. and Burgoyne, R.D. (2010) Evidence for an interaction between Golli and STIM1 in store-operated calcium entry. *Biochem. J.*, **430**, 453–460.
14. Zeiger, W., Ito, D., Swetlik, C., Oh-hora, M., Villereal, M.L. and Thinakaran, G. (2011) Stanniocalcin 2 is a negative modulator of store-operated calcium entry. *Mol. Cell Biol.*, **31**, 3710–3722.
15. Prakriya, M. (2009) The molecular physiology of CRAC channels. *Immunol. Rev.*, **231**, 88–98.
16. Zweifach, A. and Lewis, R.S. (1995) Slow calcium-dependent inactivation of depletion-activated calcium current. Store-dependent and -independent mechanisms. *J. Biol. Chem.*, **270**, 14445–14451.
17. Zweifach, A. and Lewis, R.S. (1995) Rapid inactivation of depletion-activated calcium current (I_{CRAC}) due to local calcium feedback. *J. Gen. Physiol.*, **105**, 209–226.
18. Mullins, F.M., Park, C.Y., Dolmetsch, R.E. and Lewis, R.S. (2009) STIM1 and calmodulin interact with Orai1 to induce Ca^{2+}-dependent inactivation of CRAC channels. *Proc. Natl Acad. Sci. USA*, **106**, 15495–15500.
19. Palty, R., Raveh, A., Kaminsky, I., Meller, R. and Reuveny, E. (2012) SARAF inactivates the store operated calcium entry machinery to prevent excess calcium refilling. *Cell*, **149**, 425–438.
20. Liu, X. and Ambudkar, I.S. (2001) Characteristics of a store-operated calcium-permeable channel: sarcoendoplasmic reticulum calcium pump function controls channel gating. *J. Biol. Chem.*, **276**, 29891–29898.
21. Jousset, H., Frieden, M. and Demaurex, N. (2007) STIM1 knockdown reveals that store-operated Ca^{2+} channels located close to sarco/endoplasmic Ca^{2+} ATPases (SERCA) pumps silently refill the endoplasmic reticulum. *J. Biol. Chem.*, **282**, 11456–11464.
22. Sampieri, A., Zepeda, A., Asanov, A. and Vaca, L. (2009) Visualizing the store-operated channel complex assembly in real time: identification of SERCA2 as a new member. *Cell Calcium*, **45**, 439–446.
23. Gilabert, J.A. and Parekh, A.B. (2000) Respiring mitochondria determine the pattern of activation and inactivation of the store-operated Ca(2+) current I(CRAC). *EMBO J.*, **19**, 6401–6407.
24. Hoth, M., Button, D.C. and Lewis, R.S. (2000) Mitochondrial control of calcium-channel gating: a mechanism for sustained signaling and transcriptional activation in T lymphocytes. *Proc. Natl Acad. Sci. USA.*, **97**, 10607–10612.
25. Bautista, D.M., Hoth, M. and Lewis, R.S. (2002) Enhancement of calcium signalling dynamics and stability by delayed modulation of the plasma-membrane calcium-ATPase in human T cells. *J. Physiol.*, **541**, 877–894.
26. Patergnani, S., Suski, J.M., Agnoletto, C., Bononi, A., Bonora, M., De, M.E., Giorgi, C., Marchi, S., Missiroli, S. and Poletti, F., *et al.* (2011) Calcium signaling around mitochondria associated membranes (MAMs). *Cell Commun. Signal.*, **9**, 19 19.
27. Csordas, G. and Hajnoczky, G. (2001) Sorting of calcium signals at the junctions of endoplasmic reticulum and mitochondria. *Cell Calcium.*, **29**, 249–262.
28. Hjelmqvist, L., Tuson, M., Marfany, G., Herrero, E., Balcells, S. and Gonzalez-Duarte, R. (2002) ORMDL proteins are a conserved new family of endoplasmic reticulum membrane proteins. *Genome Biol.*, **3**, RESEARCH0027.
29. Cantero-Recasens, G., Fandos, C., Rubio-Moscardo, F., Valverde, M.A. and Vicente, R. (2010) The asthma-associated ORMDL3 gene product regulates endoplasmic reticulum-mediated calcium signaling and cellular stress. *Hum. Mol. Genet.*, **19**, 111–121.
30. McGovern, D.P., Gardet, A., Torkvist, L., Goyette, P., Essers, J., Taylor, K.D., Neale, B.M., Ong, R.T., Lagace, C. and Li, C., *et al.* (2010) Genome-wide association identifies multiple ulcerative colitis susceptibility loci. *Nat. Genet.*, **42**, 332–337.
31. Moffatt, M.F., Kabesch, M., Liang, L., Dixon, A.L., Strachan, D., Heath, S., Depner, M., von Berg, A., Bufe, A. and Rietschel, E., *et al.* (2007)

Genetic variants regulating ORMDL3 expression contribute to the risk of childhood asthma. *Nature*, **448**, 470–473.
32. Barrett, J.C., Hansoul, S., Nicolae, D.L., Cho, J.H., Duerr, R.H., Rioux, J.D., Brant, S.R., Silverberg, M.S., Taylor, K.D., Barmada, M.M. *et al.* (2008) Genome-wide association defines more than 30 distinct susceptibility loci for Crohn's disease. *Nat. Genet.*, **40**, 955–962.
33. Barrett, J.C., Clayton, D.G., Concannon, P., Akolkar, B., Cooper, J.D., Erlich, H.A., Julier, C., Morahan, G., Nerup, J. and Nierras, C., *et al.* (2009) Genome-wide association study and meta-analysis find that over 40 loci affect risk of type 1 diabetes. *Nat. Genet.*, **41**, 703–707.
34. Sokol, C.L., Barton, G.M., Farr, A.G. and Medzhitov, R. (2008) A mechanism for the initiation of allergen-induced T helper type 2 responses. *Nat. Immunol.*, **9**, 310–318.
35. Lehuen, A., Diana, J., Zaccone, P. and Cooke, A. (2010) Immune cell crosstalk in type 1 diabetes. *Nat. Rev. Immunol.*, **10**, 501–513.
36. Hardenberg, G., Steiner, T.S. and Levings, M.K. (2011) Environmental influences on T regulatory cells in inflammatory bowel disease. *Semin. Immunol.*, **23**, 130–138.
37. Feske, S., Gwack, Y., Prakriya, M., Srikanth, S., Puppel, S.H., Tanasa, B., Hogan, P.G., Lewis, R.S., Daly, M. and Rao, A. (2006) A mutation in Orai1 causes immune deficiency by abrogating CRAC channel function. *Nature*, **441**, 179–185.
38. Vig, M., Peinelt, C., Beck, A., Koomoa, D.L., Rabah, D., Koblan-Huberson, M., Kraft, S., Turner, H., Fleig, A., Penner, R. and Kinet, J.P. (2006) CRACM1 is a plasma membrane protein essential for store-operated Ca^{2+} entry. *Science*, **312**, 1220–1223.
39. Zhang, S.L., Yeromin, A.V., Zhang, X.H., Yu, Y., Safrina, O., Penna, A., Roos, J., Stauderman, K.A. and Cahalan, M.D. (2006) Genome-wide RNAi screen of Ca(2+) influx identifies genes that regulate Ca(2+) release-activated Ca(2+) channel activity. *Proc. Natl Acad. Sci. USA*, **103**, 9357–9362.
40. Breslow, D.K., Collins, S.R., Bodenmiller, B., Aebersold, R., Simons, K., Shevchenko, A., Ejsing, C.S. and Weissman, J.S. (2010) Orm family proteins mediate sphingolipid homeostasis. *Nature*, **463**, 1048–1053.
41. Han, S., Lone, M.A., Schneiter, R. and Chang, A. (2010) Orm1 and Orm2 are conserved endoplasmic reticulum membrane proteins regulating lipid homeostasis and protein quality control. *Proc. Natl Acad. Sci. USA*, **107**, 5851–5856.
42. Oh-hora, M., Yamashita, M., Hogan, P.G., Sharma, S., Lamperti, E., Chung, W., Prakriya, M., Feske, S. and Rao, A. (2008) Dual functions for the endoplasmic reticulum calcium sensors STIM1 and STIM2 in T cell activation and tolerance. *Nat. Immunol.*, **9**, 432–443.
43. Muik, M., Frischauf, I., Derler, I., Fahrner, M., Bergsmann, J., Eder, P., Schindl, R., Hesch, C., Polzinger, B., Fritsch, R. *et al.* (2008) Dynamic coupling of the putative coiled-coil domain of ORAI1 with STIM1 mediates ORAI1 channel activation. *J. Biol. Chem.*, **283**, 8014–8022.
44. Montalvo, G.B., Artalejo, A.R. and Gilabert, J.A. (2006) ATP from subplasmalemmal mitochondria controls Ca^{2+}-dependent inactivation of CRAC channels. *J. Biol. Chem.*, **281**, 35616–35623.
45. Lis, A., Peinelt, C., Beck, A., Parvez, S., Monteilh-Zoller, M., Fleig, A. and Penner, R. (2007) CRACM1, CRACM2, and CRACM3 are store-operated Ca^{2+} channels with distinct functional properties. *Curr. Biol.*, **17**, 794–800.
46. Hoth, M., Fanger, C.M. and Lewis, R.S. (1997) Mitochondrial regulation of store-operated calcium signaling in T lymphocytes. *J. Cell Biol.*, **137**, 633–648.
47. Duchen, M.R. (1999) Contributions of mitochondria to animal physiology: from homeostatic sensor to calcium signalling and cell death. *J. Physiol*, **516**(Pt 1), 1–17.
48. Montero, M., Lobaton, C.D., Hernandez-Sanmiguel, E., Santodomingo, J., Vay, L., Moreno, A. and Alvarez, J. (2004) Direct activation of the mitochondrial calcium uniporter by natural plant flavonoids. *Biochem. J.*, **384**, 19–24.
49. Nagai, T., Sawano, A., Park, E.S. and Miyawaki, A. (2001) Circularly permuted green fluorescent proteins engineered to sense Ca^{2+}. *Proc. Natl Acad. Sci. USA.*, **98**, 3197–3202.
50. de la Fuente, S., Fonteriz, R.I., Montero, M. and Alvarez, J. (2012) Dynamics of mitochondrial [Ca(2+)] measured with the low-Ca(2+)-affinity dye rhod-5N. *Cell Calcium*, **51**, 65–71.
51. Cantero-Recasens, G., Gonzalez, J.R., Fandos, C., Duran-Tauleria, E., Smit, L.A., Kauffmann, F., Anto, J.M. and Valverde, M.A. (2010) Loss of function of transient receptor potential vanilloid 1 (TRPV1) genetic variant is associated with lower risk of active childhood asthma. *J. Biol. Chem.*, **285**, 27532–27535.
52. Valverde, M.A., Cantero-Recasens, G., Garcia-Elias, A., Jung, C., Carreras-Sureda, A. and Vicente, R. (2011) Ion channels in asthma. *J. Biol. Chem.*, **286**, 32877–32882.
53. Oh-hora, M. and Rao, A. (2008) Calcium signaling in lymphocytes. *Curr. Opin. Immunol.*, **20**, 250–258.
54. Ranger, A.M., Oukka, M., Rengarajan, J. and Glimcher, L.H. (1998) Inhibitory function of two NFAT family members in lymphoid homeostasis and Th2 development. *Immunity*, **9**, 627–635.
55. Sommers, C.L., Park, C.S., Lee, J., Feng, C., Fuller, C.L., Grinberg, A., Hildebrand, J.A., Lacana, E., Menon, R.K. and Shores, E.W., *et al.* (2002) A LAT mutation that inhibits T cell development yet induces lymphoproliferation. *Science*, **296**, 2040–2043.
56. Aguado, E., Richelme, S., Nunez-Cruz, S., Miazek, A., Mura, A.M., Richelme, M., Guo, X.J., Sainty, D., He, H.T., Malissen, B. and Malissen, M. (2002) Induction of T helper type 2 immunity by a point mutation in the LAT adaptor. *Science*, **296**, 2036–2040.
57. Lur, G., Haynes, L.P., Prior, I.A., Gerasimenko, O.V., Feske, S., Petersen, O.H., Burgoyne, R.D. and Tepikin, A.V. (2009) Ribosome-free terminals of rough ER allow formation of STIM1 puncta and segregation of STIM1 from IP(3) receptors. *Curr. Biol.*, **19**, 1648–1653.
58. Rizzuto, R., Pinton, P., Carrington, W., Fay, F.S., Fogarty, K.E., Lifshitz, L.M., Tuft, R.A. and Pozzan, T. (1998) Close contacts with the endoplasmic reticulum as determinants of mitochondrial Ca^{2+} responses. *Science*, **280**, 1763–1766.
59. Montero, M., Alonso, M.T., Carnicero, E., Cuchillo-Ibanez, I., Albillos, A., Garcia, A.G., Garcia-Sancho, J. and Alvarez, J. (2000) Chromaffin-cell stimulation triggers fast millimolar mitochondrial Ca2+ transients that modulate secretion. *Nat. Cell Biol.*, **2**, 57–61.
60. Watson, R. and Parekh, A.B. (2012) Mitochondrial regulation of CRAC channel-driven cellular responses. *Cell Calcium*.
61. Quintana, A. and Hoth, M. (2012) Mitochondrial dynamics and their impact on T cell function. *Cell Calcium*, **52**, 57–63.
62. Quintana, A., Schwarz, E.C., Schwindling, C., Lipp, P., Kaestner, L. and Hoth, M. (2006) Sustained activity of calcium release-activated calcium channels requires translocation of mitochondria to the plasma membrane. *J. Biol. Chem.*, **281**, 40302–40309.
63. Quintana, A., Pasche, M., Junker, C., Al-Ansary, D., Rieger, H., Kummerow, C., Nunez, L., Villalobos, C., Meraner, P. and Becherer, U., *et al.* (2011) Calcium microdomains at the immunological synapse: how ORAI channels, mitochondria and calcium pumps generate local calcium signals for efficient T-cell activation. *EMBO J.*, **30**, 3895–3912.
64. Singaravelu, K., Nelson, C., Bakowski, D., de Brito, O.M., Ng, S.W., Di, C.J., Powell, T., Scorrano, L. and Parekh, A.B. (2011) Mitofusin 2 regulates STIM1 migration from the Ca^{2+} store to the plasma membrane in cells with depolarized mitochondria. *J. Biol. Chem.*, **286**, 12189–12201.
65. Landolfi, B., Curci, S., Debellis, L., Pozzan, T. and Hofer, A.M. (1998) Ca^{2+} homeostasis in the agonist-sensitive internal store: functional interactions between mitochondria and the ER measured In situ in intact cells. *J. Cell Biol.*, **142**, 1235–1243.
66. Roelants, F.M., Breslow, D.K., Muir, A., Weissman, J.S. and Thorner, J. (2011) Protein kinase Ypk1 phosphorylates regulatory proteins Orm1 and Orm2 to control sphingolipid homeostasis in Saccharomyces cerevisiae. *Proc. Natl Acad. Sci. USA*, **108**, 19222–19227.
67. Liu, M., Huang, C., Polu, S.R., Schneiter, R. and Chang, A. (2012) Regulation of sphingolipid synthesis via Orm1 and Orm2 in yeast. *J. Cell Sci.*, **125**, 2428–2435.
68. Sun, Y., Miao, Y., Yamane, Y., Zhang, C., Shokat, K.M., Takematsu, H., Kozutsumi, Y. and Drubin, D.G. (2012) Orm protein phosphoregulation mediates transient sphingolipid biosynthesis response to heat stress via the Pkh-Ypk and Cdc55-PP2A pathways. *Mol. Biol. Cell.*, **23**, 2388–2398.
69. Arniges, M., Vazquez, E., Fernandez-Fernandez, J.M. and Valverde, M.A. (2004) Swelling-activated Ca^{2+} entry via TRPV4 channel is defective in cystic fibrosis airway epithelia. *J. Biol. Chem.*, **279**, 54062–54068.